Behavior of FGM-coated, HA-Coated and Uncoated Femoral Prostheses with Different Geometrical Configurations

Tawakol A. Enab
Production Engineering and Mechanical Design Department, Faculty of Engineering, Mansoura University, P.O. 35516 Mansoura, Egypt. Tel.: +201094684833, Fax: +20502244690, Emails: tenab@mans.edu.eg ; tewmkaln@yahoo.com

***Abstract*— Maintaining interface stresses within the adequate levels while minimizing the stress shielding in the prosthesis surrounding bone consider a design challenge in total hip replacement.Functionally graded materials (FGMs), coatings and hip femoral stem designs considered as the most important concepts used for this purpose. The current investigation compares the biomedical performance of these three concepts. Five femoral stem material cases were studied for three different stem geometrical configurations. These cases include uncoated titanium stem, vertically distributedFGM stem, Ti-stem with homogenous hydroxyapatite coating and Ti-stem with FGM coatings distributedradially and vertically.Titanium and hydroxyapatite are the principal constituents' of FGMs. Five FGM composition variation control parameters (*m* = 0.1, 0.5, 1, 2, 10) were considered in FGM cases. Moreover, threecoating thicknesses (100 µm, 300 µm and 500 µm) employed for coated stem cases.The results revealed that, the values and distributions of shear stresses at different interfaces and von Mises stressesdeveloped at femoral stems, cement and bone vary from one prosthesis profile to another. Furthermore, vertically distributed FGM stem develops the lower stresses in the femoral prosthesis and the higher stresses in bone which will reduce the stress shielding and will increase the lifespan of the total hip replacement.**

***Index Term*-- Total hip replacement; Femoral prosthesis; Functionally Graded Material (FGM), Coating; Finite element analysis; Stress shielding.**

I. Introduction

The development of new hip joint implants is a challenge to improve their actual performance and success rates. Cobalt-chromium (Co-Cr) alloys, titanium (Ti) and its alloys, Ti-6Al-4V and stainless steel (SS) are frequently used as implants due to their good corrosion resistance and reasonable fatigue life properties. Currently, titanium and its alloys considered as the most important materials for artificial joints since their mechanical properties are closer to those of natural bone than are those of Co-Cr alloys or SS. But in general, these metallic materials are much stiffer than cortical bone. Consequently, potential proximal stress shielding and bone resorption may occur which may lead to prosthesis failure or may require revision surgery [1-3].

Since for a given stem geometry design, prosthesis material elastic modulus consider as the most critical design variable. Because, it essentially controls how the load is transferred to the surrounding bones of artificial joint [4]. Thus, some concepts of femoral stems with graded flexibility were proposed to mitigate the stress shielding effect and the other negative effects. Some techniques for material optimization of hip stems through one and two-dimensional functionally graded material (FGM) suggested by Hedia et al. [5-7]. Their proposed techniques showed that the use of FGM stems reduce the stress shielding at the proximal lateral bone and the maximum interface shear stress at the femoral stem/bone interface compared to homogenous titanium stem. Also, Al-Jassir et al. [8] showed that using functionally graded stem increases the resultant stresses at the femur bone compared to metallic stem which will reduces the stress shielding effects.

Furthermore, different geometrical configurations of functionally graded femoral prostheses (FGFPs) studied by Oshkour et al. [9-14]using three-dimensional finite element analysis. They concluded that, stress shielding and interface stress can decreased by the employment of femoral prosthesis with adjustable stiffness (i.e. FGFPs), which result in an increase in the total lifespan of the hip replacement. Moreover, Lopes et al. [15] introduce a new concept for a femoral stem through a graded elastic modulus using metastable β-Ti alloy. Their results confirmed the feasibility of designing biomedical implants with hybrid mechanical behavior from metastable β-Ti alloys. They attained a stem with an adjustable elastic modulus (***E*** varying from 65 GPa to 110 GPa) by applying specific heat treatments to specific regions in the femoral stem.

Additionally nowadays, coatings materials are broadly used in industrial applications to provide valuable improvements in designs. These improvements may be against wear, corrosion, erosion, heat, etc. [16]. Therefore, coated stems may be used as another concept to reduce stress shielding and interface stresses restrictions. Hydroxyapatite (HA) attracted attention as a surface-coating compound as a result of its high osteoconductivity since it considered as the main inorganic component in the mammal bone or tooth [2]. Chambers et al. [17] evaluated the clinical use of tapered cementless femoral stems with hydroxyapatite coating. They revealed that, hydroxyapatite-coated femoral stems had a considerable improvement on the proximal femoral fixation. This improvement reflected radiographically by more bone growth around the implant proximal portion and less proximal stress shielding.

A review of material fundamentals and clinical performance of plasma-sprayed hydroxyapatite coatings carried out by Sun et al. [1]. Moreover, Park et al. [18] study of the clinical and radiographic results of using plasma spray-coated Ti femoral component for cementless total hip arthroplasty. They concluded that, femoral stems with plasma-sprayed HA coatings revealed advantages of faster and stronger fixation and higher osseous remodeling both in vivo and clinically. Furthermore, several investigations studied the synthesis and the advantages of using hydroxyapatite (HA), calcium silicate (CS) ceramics and other bioactive-coatings deposited on femoral stems in total hip arthroplasty [19-27].

Evans and Gregson [28] suggested a numerical optimization technique to improve the design of a coated, cementless hip prosthesis. They represented the prosthesis by a simple one-dimensional finite element model. They retained implant-bone interface stresses within normal limits and minimized stress shielding by altering implant diameter and coating thickness at various points. Their proposed design showed a noticeable reduction in interface stresses and stress shielding compared to traditional designs. Moreover, a 3D-FEM model of biocomposite metal-surface coating system consists of Ti6Al4V metallic substrate and hydroxyapatite (HA) coating proposed by Sobieszczyk et al. [29] and used to estimate the behavior of biocomposite metal-surface coating systems influenced by external loading.

Recently, Hedia and Fouda gathered the functionally graded material and coating concepts in their investigations of cement and cementless hip prostheses [30, 31]. They found that, femoral stems coated with functionally graded hydroxyapatite and collagen significantly reduce stress shielding compared to homogenous titanium stem coated with hydroxyapatite [31]. Moreover, they investigated the use of FGM coating on retreating stress shielding at the medial proximal region of the femur. They graded the elastic modulus of the coating material vertically from hydroxyapatite at the stem proximal part (top) and collagen at the distal end of the stem (bottom). They concluded that, femoral stem with FGM coating demonstrated an increasing of maximum von Mises stress at the medial proximal region of the femur bone compared to titanium stem and titanium stem coated with HAP, respectively [30]. As a result of FGM coating, a reduction in the stress shielding obtained which lead to prevent bone resorption. But, they carried out their investigations on a single stem geometry design. However, the stem geometry design plays an important role on stress distribution in total hip replacement as indicated by several researches [32-42]. Additionally, it is worth to note that, Oshkour et al. [9, 10, 14] in their investigations taken into account the functionally graded material and different geometrical configurations of femoral prostheses. They accomplished their comparative studies about the performance of longitudinal and radial functionally graded femoral stems with different geometrical configurations through three-dimensional finite element analyses.

Consequently, to the best of the author's knowledge, past investigations focusing only on one or in the best case two of the aforementioned concepts (i.e. the functionally graded materials, the coating and the different hip femoral stem designs). Therefore, the main objective of the current investigation is the employment of the abovementioned concepts to evaluate their effects on stress distributions in cemented total hip replacement using two-dimensional finite element analysis. Moreover, the present work set out to explore the best way of using these concepts to reduce the stress shielding occurred in the femur bone after prosthesis implantation as well as interface stress between the implant and bone.

II. MATERIALS AND METHODS

A. *Functionally graded material (FGM)*

Currently, the development of new biomaterials for medical applications considered as the most challenging task for biomaterials researchers. Moreover, complex hierarchical structures are notable feature of natural biomaterials such as bone. Consequently, functionally graded materials (FGMs) used as synthetic biomaterials with controlled hierarchical structures, which can resemble the natural ones. They proposed to satisfy the obvious need for better artificial dental [43-45], hip [5, 7-14, 30, 31] and knee [46-50] implants.

The two-components FGM considered in this study can be described by a compositional gradient from one component to the other. Constituents' volume fractions vary gradually in some directions as a function of position resulting in corresponding changes in the properties of the material. Thus, the volume fractions of the constitutive materials (i.e. material 1 and material 2) characterized by V1 and V2 respectively. These volume fractions represented by the following equations [6, 46-48, 51]:

$$V_1 = \left(\frac{y}{h}\right)^m \tag{1}$$

$$V_2 = \left(1 - V_1\right) \tag{2}$$

where***h*** denotes the total height of the FGM in the gradation direction, ***y*** denotes the position of different gradation points along it and ***m*** is a parameter that controls the composition variation through it. For FGM with material 1 rich composition parameter ***m*** must be less than unity. While, for FGM with material 2 rich composition parameter m must be greater than unity. The FGM porosity ***p*** may be calculated using the following equation [51]:

$$p = A\left(\frac{y}{h}\right)^n \left[1 - \left(\frac{y}{h}\right)^z\right] \tag{3}$$

where $$0 \le A \le \frac{((n+z)/n)^n}{1-(n/(n+z))^z} \tag{4}$$

The arbitrary parameters ***A***, ***n*** and ***z*** control the FGM porosity and taken as 0.1, 1 and 1 respectively [46-48]. The effective modulus of elasticity at any point within the FGM can be represented by the following relationships [51]:

$$E = \frac{E_O(1-p)}{1+\dfrac{p(5+8\nu)(37-8\nu)}{8(1+\nu)(23+8\nu)}} \tag{5}$$

where $$E_O = E_2\left[\frac{E_2+(E_1-E_2)V_1^{2/3}}{E_2+(E_1-E_2)(V_1^{2/3}-V_1)}\right] \quad (6)$$

$$\nu = \nu_1 V_1 + \nu_2 V_2 \quad (7)$$

Noting that, $\boldsymbol{E_0}$ denotes the elastic modulus at zero porosity, $\boldsymbol{E_1}$, $\boldsymbol{E_2}$ and $\boldsymbol{\nu_1}$, $\boldsymbol{\nu_2}$ are the elastic moduli and Poisson's ratios of the two constitutive materials, respectively.

B. Femur and prosthesis models

In fact, as indicated above numerous studies tried to enhance hip prosthesis implant stiffness by altering its geometry and material to accomplish greater compatibility between the implant and femur. The current investigation considers only the three hip prosthesis implant profiles proposed by Oshkour et al. [9, 10, 14] (Fig. 1). For simplicity, the comparative studies will only conducted on two dimensional models of the proposed profiles using finite element method. The following five case studies will considered for cemented hip femoral stems:

- Case 1 (***Ti-uncoated***): uncoated titanium stem
- Case 2 (***FGMV stem***): vertically distributed functionally graded material stem
- Case 3 (***Ti-HA coat***): titanium stem with hydroxyapatite coating
- Case 4 (***Ti-FGMR coat***): titanium stem with radially distributed functionally graded material coating
- Case 5 (***Ti-FGMV coat***): titanium stem with verticallydistributed functionally graded material coating

Coating thickness has a very important role on the performance of the metallic medical implants [20, 23, 29-31, 52]. Some of the pervious literatures used femoral stems with coating thickness in the range of 100µm to 500 µm [30, 31]. Therefore, in the current research three coating thicknesses (100 µm, 300 µm and 500 µm) employed for each stem with coating material (cases 3, 4, and 5). Moreover, five FGM composition variation control parameters (***m*** = 0.1, 0.5, 1, 2, 10) considered for FGM stem (case2) and stems with FGM coating (cases 4 and 5). Accordingly, 117 femoral prostheses models were employed to conduct this numerical study.

C. Finite element modeling of hip implants

Finite element analysis (FEA) frequently used to study the biomechanical performance of hip joint implant designs as well as to explore the effect of various parameters on implant success. Furthermore, FEA used to optimize design and materials selection in many load-bearing components. ANSYS general purpose FEAs package used to construct, run and get results from the 2D models of the above aforementioned cases. For this purpose, ANSYS parametric design language (APDL) used to facilitate the studying the influence of different parameters on stress shielding arising in the implanted joint. Therefore, each model is a construction consists of the hip-joint prostheses anchored in the resected proximal femur with poly-methyl-methacrylate (PMMA) bone cement. Thus, all models include cortical bone, cancellous bone, PMMA bone cement and femoral stem (Fig. 2).

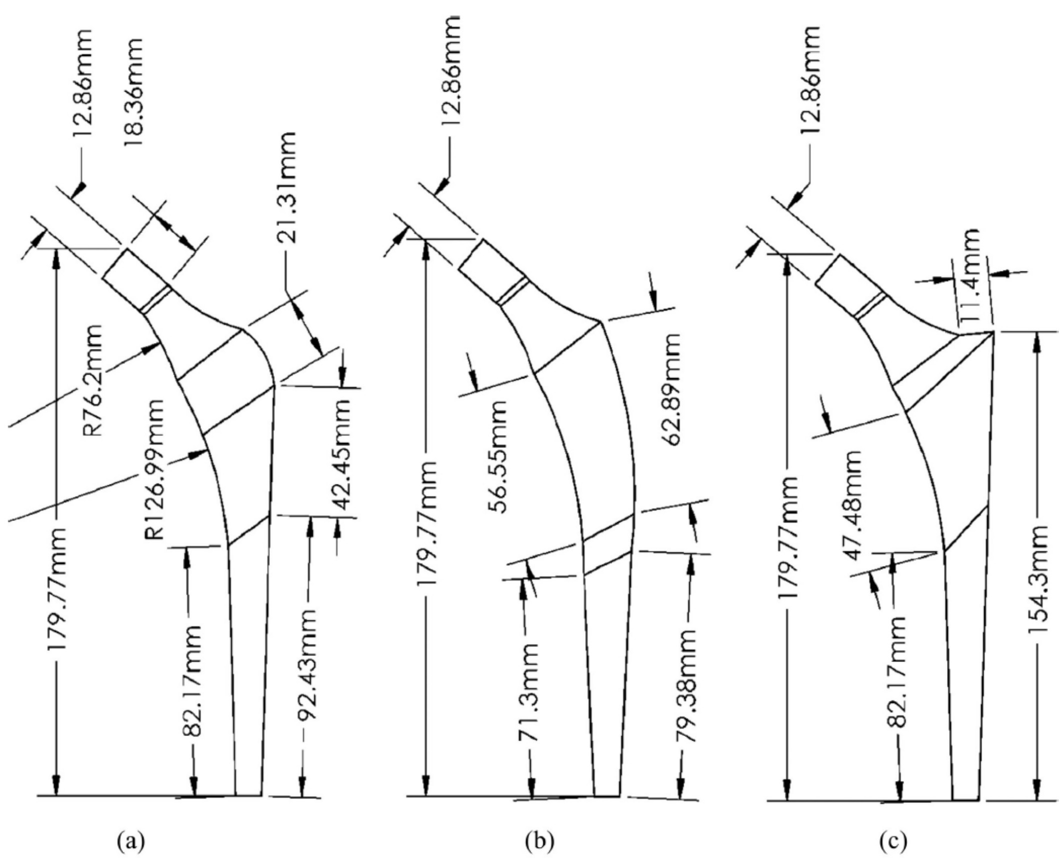

Fig. 1.Hip prosthesis profiles: (a) 1st profile, (b) 2nd profile, (c) 3rd profile after [9, 10, 14].

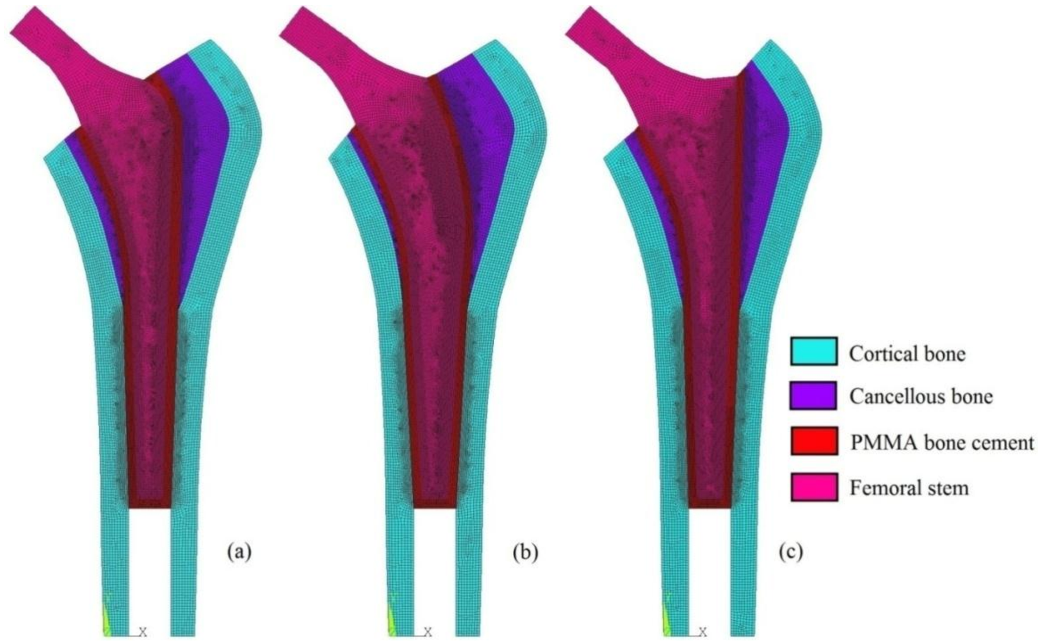

Fig. 2. The finite element models of the uncoated hip prosthesis profiles (case 1) showing the different materials ((a) 1st profile, (b) 2nd profile and (c) 3rd profile).

Mechanical properties of cortical bone, cancellous bone, PMMA bone cement, titanium femoral stem as well as FGM constitutes taken from literatures [9, 10, 13, 14]. Noting that, except cortical bone all materials considered to be isotropic, linearly elastic and homogeneous. Moreover, titanium and hydroxyapatite used as the metallic and ceramic constitutes of the FGM femoral stem and FGM coatings. However, the volume fractions of the constituent materials and thus the gradation of the mechanical properties were controlled by the FGM composition variation parameter $\boldsymbol{m}$. As indicated above, five FGM composition variation control parameters ($\boldsymbol{m}$ = 0.1, 0.5, 1, 2, 10) considered for FGM stems and stems with FGM coating. Figure 3 presents the variation in the elastic modulus for different FGM composition variation control parameter ($\boldsymbol{m}$). Noting that, elastic modulus variation will be throughout the prosthesis length for FGM stems (case 2) and stems with vertically distributed FGM coating (case 5) and will be throughout the coating thickness for stems with radially distributed FGM coating (case 4). Table (1) shows the mechanical characteristics of biological and biomaterials used in the developed models.

C.1. Application of material gradient

FGM simulation must reveal the graded distribution of material properties. Important efforts paid to precisely attain continuous property variation into finite element formulations. In fact, ANSYS has no specified material module for the FGM analysis. On the other hand, many experimentally produced FGMs have a stepwise variation in properties and should be modeled as such [53]. Consequently, the analysis of 1D-FGM is usually based on medium segmentation into a number of layers with different material properties depending on the distribution direction (i.e. vertical or radial) and the composition variation control parameter ($\boldsymbol{m}$). Therefore, for radially distribution FGM, material properties assigned to each layer. However, in the current study free meshing was used which complicate properties assignment of FGM with vertical distribution. Thus, for FGM distributed vertically, material properties assigned to each element individually using element centroid coordinates and the FGM governing equations mentioned above. In general, the two techniques of material assignment lead to a discontinuous step-type variation in properties. But, this may compromise a more appropriate representation of a real functionally graded material than an ideal smooth gradient. Figure (4-b to 4-e) shows a close-up of meshing to illustrate the distributions of functionally graded material for the different cases.

C.2. Loading and boundary conditions

Usually, static finite element analyses (FEAs) utilized to simulate simplified loading configurations of hip prosthesis implant. These FEAs are carried out under body weight loads. In general, complex loading scenarios including a number of muscle forces as well as the hip contact force can be employed to simulate the different hip loading conditions. The simulations of hip implant and femur frequently employ muscle forces to obtain realistic approximation of the musculoskeletal loading conditions. Consequently in the present study, a load of 3000 N acting at an angle of 20º applied to the prosthesis head, which is similar to the highest gait load obtained during normal walking for a 70 kg person. Moreover, a force of 1250 N employed at an angle of 20º to the vertical over the proximal area of the greater trochanter which come close to the abductor muscle load. Finally, the ilio-tibial-tract load represented by 250 N force employed parallel to the femur shaft in the distal direction [4, 30]. Restraints applied distally to the cortical bone of the femur shaft. Locations of the applied loads and restraints are shown in Fig. (4-a).

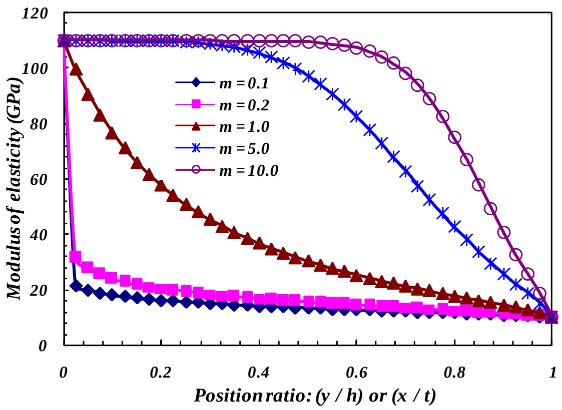

Fig. 3. Variation in the modulus of elasticity for different FGM composition variation control parameter (***m***).

Table I
Mechanical characteristics of biological and biomaterials represented in the FE models.

Material	*Plane*	*Modulus of elasticity (GPa)*	*Modulus of rigidity (GPa)*	*Poisson's ratio*
Cortical bone	*xx*	11.5	3.6	0.31
	yy	11.5	3.3	0.31
	zz	17.0	3.3	0.31
Cancellous bone	--	2.13	--	0.30
PMMA cement	--	2.7	--	0.35
Titanium (Ti)	--	110	--	0.30
Hydroxyapatite	--	10	--	0.30

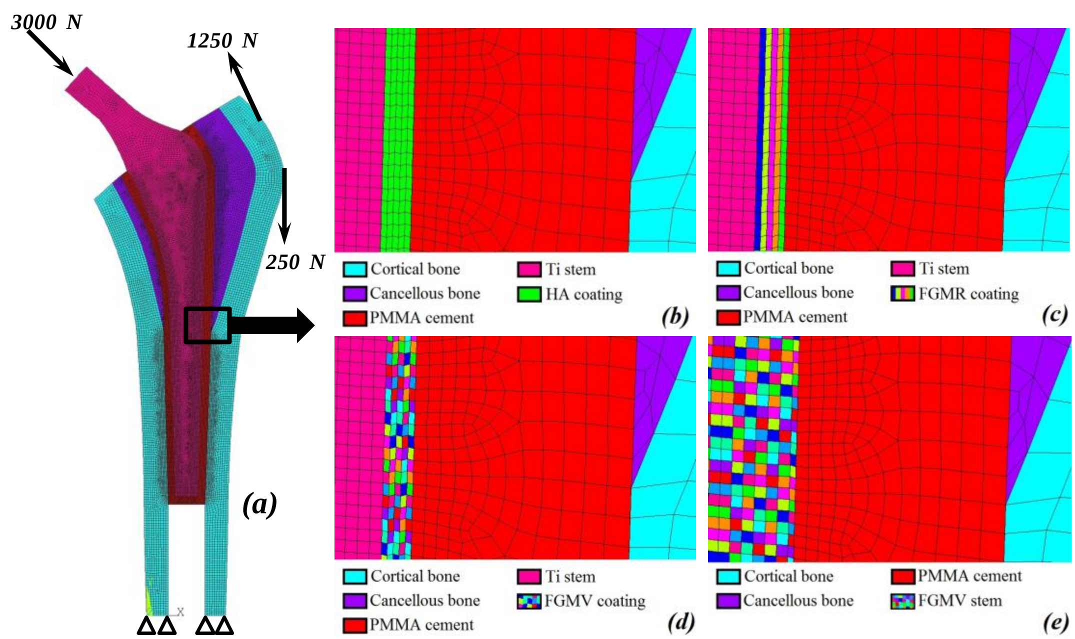

Fig. 4.The finite element model of the uncoated hip profiles (case 1) showing the applied loads and restraints ***(a)*** and close-up of meshing to illustrate the other cases: Ti-stem coated with HA coating ***(b)***, FGMR coating ***(c)***, FGMV coating ***(d)*** and FGMV stem***(e)***.

III. Results and Discussion

Precedent investigations show that mechanical properties particularly the elastic modulus of the prosthesis material is the most significant design variable which determines how load is transferred from the prosthesis to the bone via the cement [4, 47]. Since implant with high elastic modulus induce less deformation and thus lower strain energy in the bone surrounding the implant which may lead to bone stress shielding [9, 47]. Accordingly, there is a need to transfer higher stress to the implant to approach the stress levels of the normal biological bone. Moreover, coatings materials are recently applied to hip and knee prostheses to provide valuable improvements in designs. Therefore, the subsequent present the results and discussion about the effect of using different material types of femoral stems (Ti-uncoated, FGMV stem, Ti-HA coat, Ti-FGMR coat and Ti-FGMV coat) on the stresses developed in the implanted hip joint for three stem profiles.

A comparison of shear stresses distributions for stem/cement and cement/bone interfaces in lateral and medial sides for the first profile using the abovementioned five femoral stem cases presented in Fig. 5. Noting that, the composition variation control parameter (***m***) for FGMs taken as one (cases 2, 4 and 5) and for coated stems coating thickness taken as 500 μm (cases 3, 4 and 5). It can be noted that, the distal sections in stem/cement and cement/bone interfaces for both lateral and medial sides usually have the maximum shear stresses. Moreover, for both lateral and medial femoral stem/PMMA cement interfaces, shear stresses decreased gradually from distal towards the proximal.

Fig. 6 illustrates the comparison of maximum shear stresses developed at both lateral and medial sides of stem/cement and cement/bone interfaces for the five cases using the three femoral prostheses geometrical configurations, respectively. It is observed that, except at the small coating thickness (i.e. 100 μm) for the lateral stem/cement interface the ***Ti-uncoated*** case usually shows the maximum shear stresses at both lateral and medial stem/cement and lateral cement/bone interfaces. Since, for the 100 μm coating thickness ***Ti-FGMR coat*** case has the maximum lateral stem/cement interface shear stresses for the three stem profiles. Comparing to the ***Ti-uncoated*** case, maximum interface shear stresses increased by about 3% for 1st and 3rd profile and by about 4% for the 2nd profile. By contrast, ***FGMV stem*** case shows the minimum shear stresses for both lateral and medial stem/cement interfaces and lateral cement/bone interface. While, ***FGMV stem*** case usually presents the maximum shear stress at medial cement/bone interface. In addition, except ***FGMV stem*** case there is a negligible change in the maximum shear stresses values at both lateral and medial cement/bone interfaces.

Moreover, comparing the effect of the three femoral prostheses geometrical configurations on the maximum shear stresses at different interfaces, it is found that for all cases, 1st profile usually develops the maximum interfaces shear stresses while the 2nd profile frequently develops the minimum values.

Fig. 7 shows the effect of the FGM composition variation control parameter (***m***) on the maximum interface shear stresses for ***FGMV stem***, stem with ***FGMR coat*** and stem with ***FGMV coat*** cases using the three stem profiles. Noting that, for coated stems coating thickness was taken as 500 µm. It is observed that; for the 1st stem profile; the maximum shear stress values decrease by increasing the FGM composition variation control parameter (***m***) for both lateral and medial stem/cement interfaces and lateral cement bone interface. At contrast, medial cement/bone interface shows an increasing in the maximum interface shear stress by increasing FGM ***m***-parameter. Furthermore; for the 2nd and 3rd stem profiles; increasing FGM ***m***-parameter reduces the values of the maximum interface shear stresses at both lateral and medial stem/cement interfaces. While, it has a negligible effect for both lateral and medial cement/bone interfaces.This reduction in the maximum shear stress valuesmay be interpreted by the fact that higher FGM ***m***-parameter results in hydroxyapatite rich FGM coating especially at the interface region. This will help in smooth stress transferring to bone via cement mantle.

The maximum von Mises stresses developed in the cortical bone at its lateral and medial sides are shown in Fig. 8-a and b. Whereas, Fig. 8-c presents the maximum von Mises stresses developed in the three profiles configurations of femoral stems for the different cases. It obvious to note that, the variation of the maximum von Mises stresses for the different cases varies according to the different geometrical configurations of hip femoral stems.In addition, for the same femoral stem profile, the different cases show slight distinction in the values of maximum von Mises stresses developed in cortical bone in particular at its lateral side. While at its medial side,***FGMV stem*** case has significant increasing in the maximum von Mises stresses compared to the other cases.

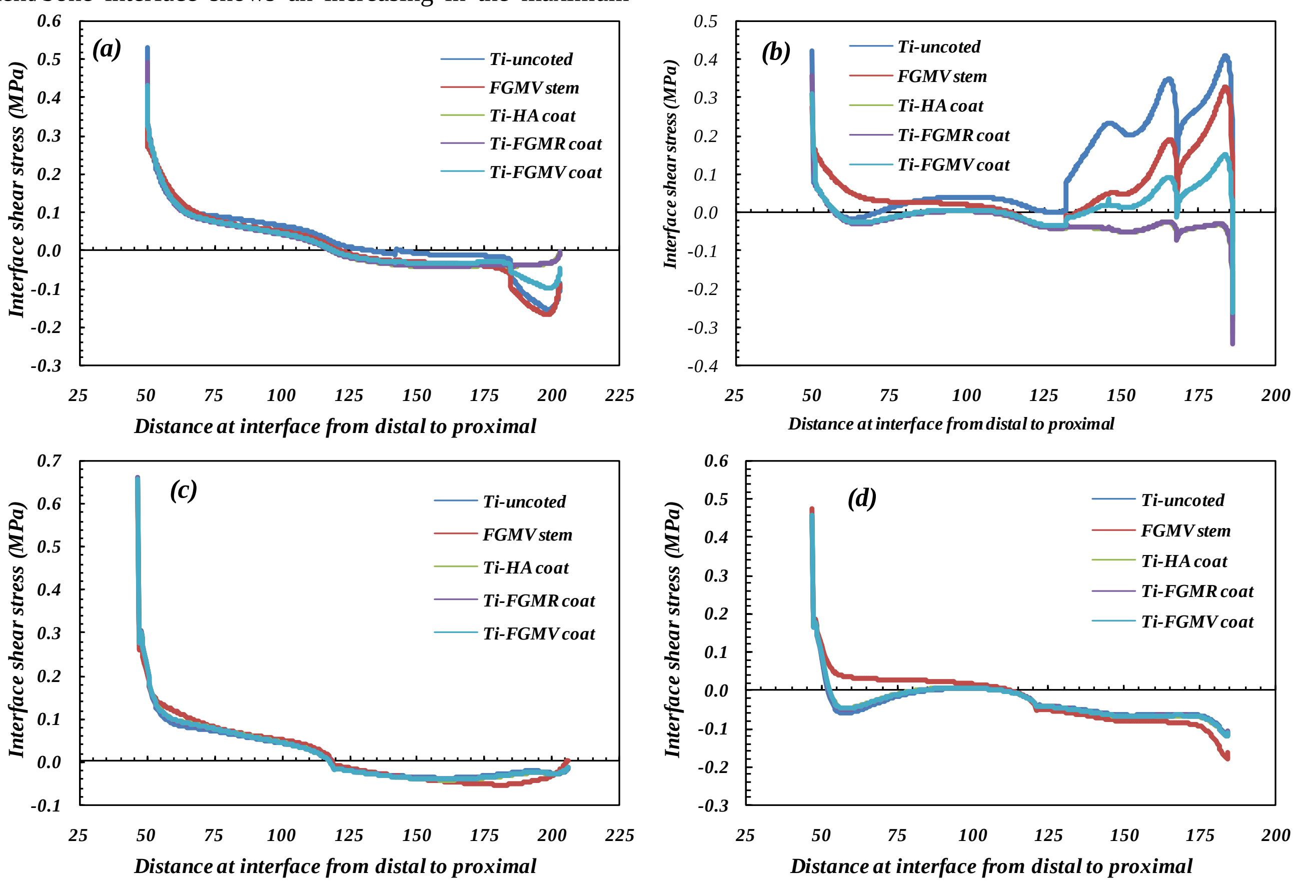

Fig. 5. Distribution of shear stresses using the first femoral stem profile along ***(a)*** lateral and ***(b)*** medial sides of stem/cement interfaces and along ***(c)*** lateral and ***(d)*** medial sides of cement/bone interfaces.

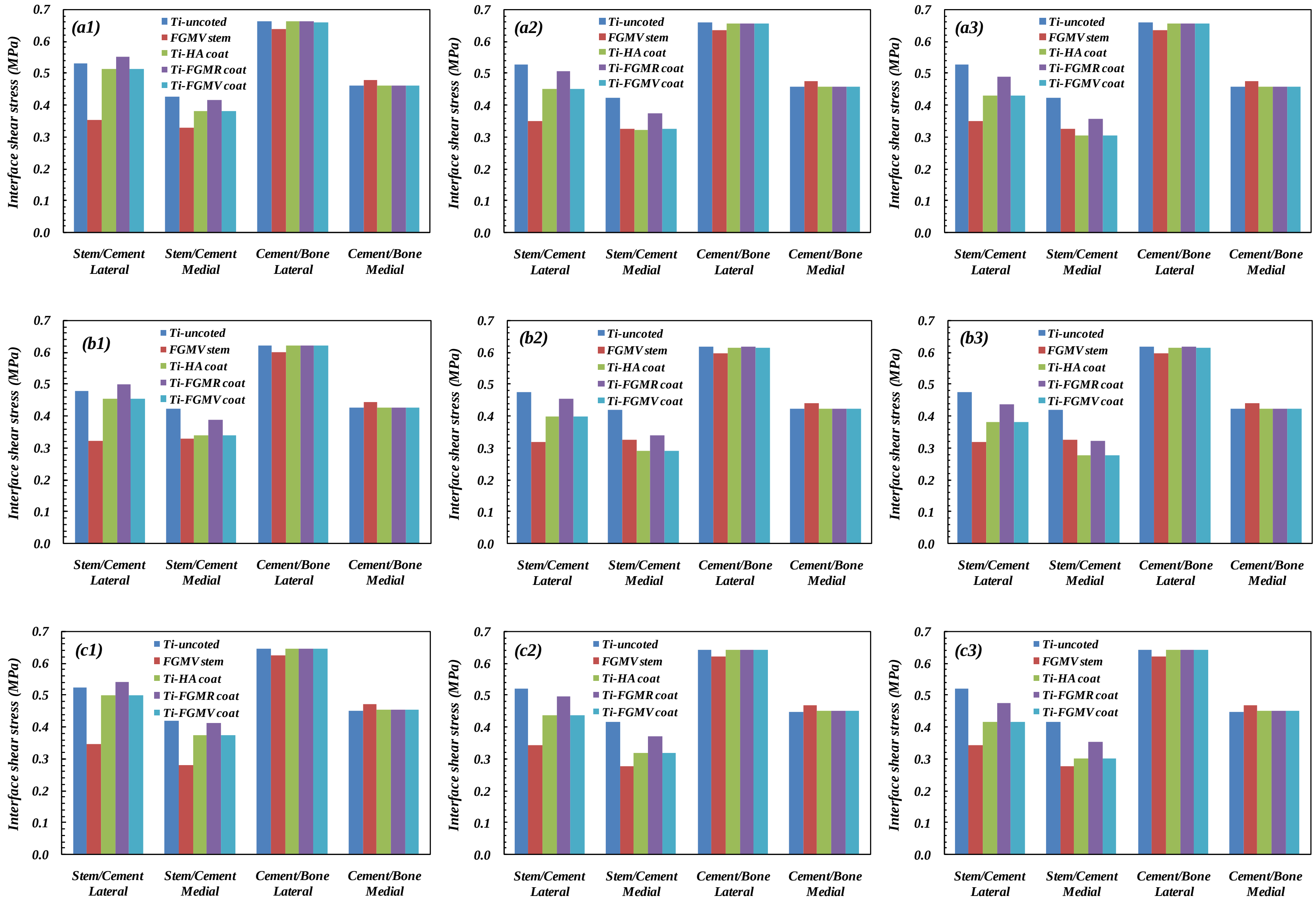

Fig. 6. Maximum interface shear stress for the different studied cases for: ***(a)*** 1st profile, ***(b)*** 2nd profile and ***(c)*** 3rd profile and for coating thicknesses of: ***(1)*** 100µm, ***(2)*** 300µm and ***(3)*** 500µm.

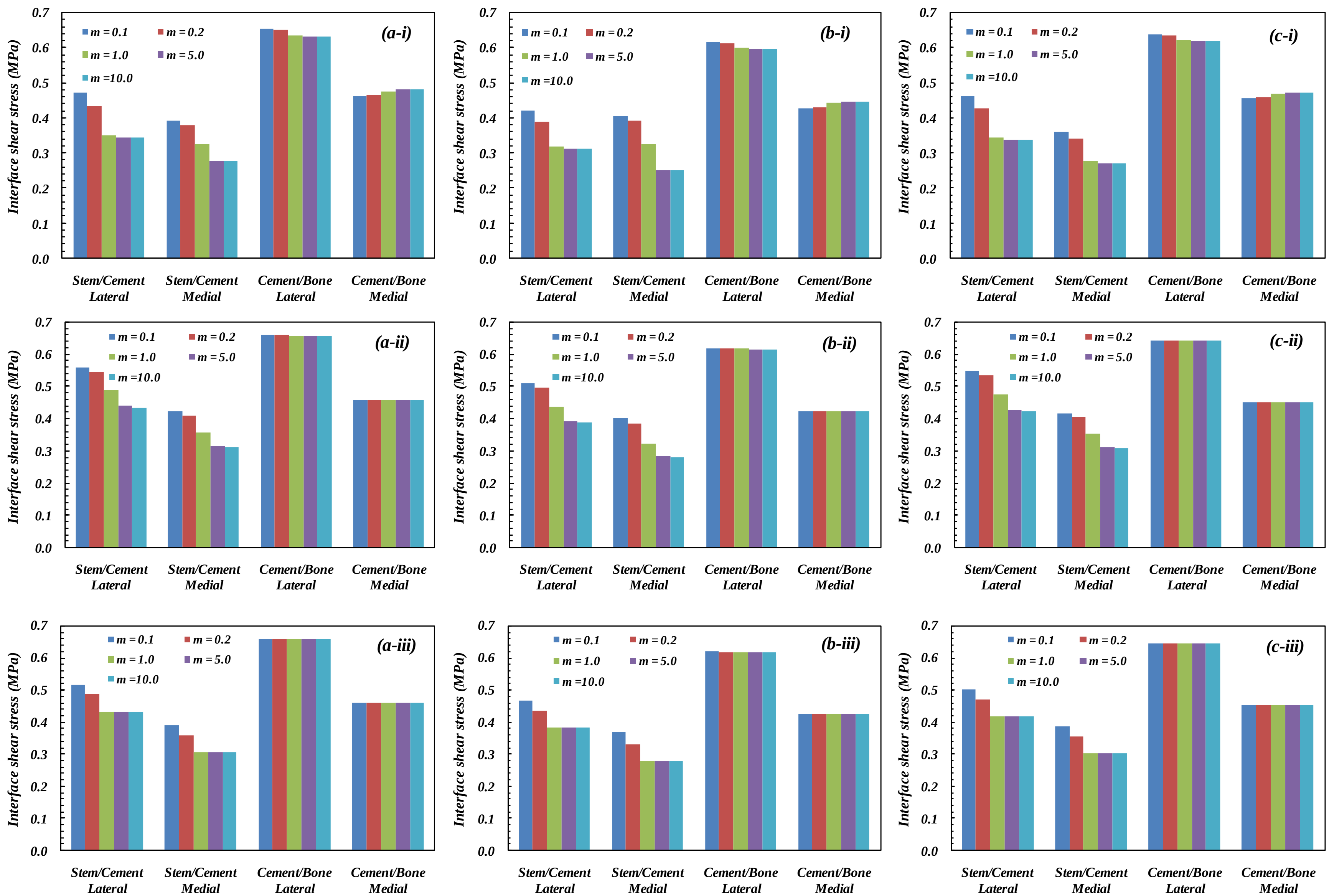

Fig. 7.Effect of composition variation control parameter (***m***) on the maximum interface shear stress for:***(a)*** 1[st] profile, ***(b)***2[nd]profile and ***(c)***3[rd] profile and for cases: ***(i)*** FGMV stem, ***(ii)*** stem with FGMR coat and ***(iii)*** stem with FGMV coatwith coat thickness of 500 μm.

On the contrary, 2nd geometrical profile usually develops the higher levels of von Mises stresses at cortical bone (Fig. 8-b) and the lower levels at femoral stems (Fig. 8-c) in all cases compared to the 1st and 3rd femoral stem profiles. Therefore, from the developed stresses point of view, femoral prostheses with 2nd profile geometrical configuration is preferred since it induce high levels of stresses in bone and low levels in femoral stem which will minimize bone stress shielding. Moreover, vertically distributed functionally graded material stem represents the most effective case compared to the other cases. Also, it is worth to note that; in addition to the geometrical configuration of the prosthesis;the FGM composition variation control parameter (***m***) can be changed to adjust the developed stresses in the implant and surrounding bone.

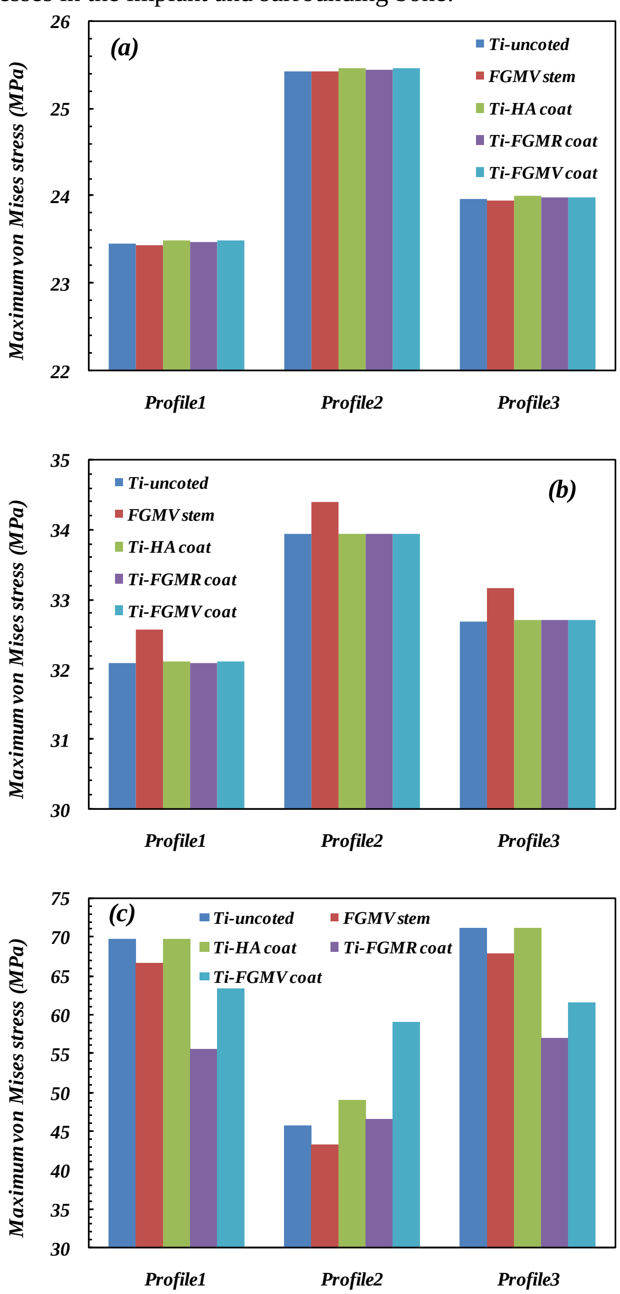

Fig. 8. Maximum von Mises stresses developed in: cortical bone at both ***(a)*** lateral and ***(b)*** medial sides and in ***(c)*** femoral stem.

IV. Conclusions

Thisstudy compared the performance of three femoral stem designs using five femoral stem material cases comprise uncoated Ti-stem, FGM stem, Ti-stem with HA coating and Ti-stem with FGM coatings distributed radially and vertically. The results of the current study lead to the following conclusions.

- Maximum shear stresses at stem/cement interface influenced significantly by the prosthesis design, coating thickness and FGM composition variation control parameter (***m***). While, they had limited variations at cement/bone interface for all combinations of profiles,coating thickness and FGM ***m***-parameter.
- The second femoral prosthesis profile usually induced high stress levels in bone and low levels in femoral stem which will minimize bone stress shielding.
- Increasing coating thickness reduced the developed von Mises stresses in the femoral stem and shear stresses at interfaces although it increased the developed von Mises stresses in the bone.
- FGM composition variation control parameter (***m***) had a considerableinfluence on developed stresses. For stems with FGM coatings, maximum shear stress values reduced by increasing FGM ***m***-parameter which will give smooth stress transferring to bone via cement mantle.
- FGMV stem induced the lower stresses in the femoral prosthesis and the higher stresses in bone compared to the other stem material cases.

Consequently, the use of functionallygraded materials in femoral stem or as coating will increase the hip prosthesis performance and life.

References

[1] L. Sun, C. C. Berndt, K. A. Gross, and A. Kucuk, "Material fundamentals and clinical performance of plasma ‐ sprayed hydroxyapatite coatings: a review," Journal of biomedical materials research, vol. 58, pp. 570-592, 2001.

[2] K. Kuroda and M. Okido, "Hydroxyapatite coating of titanium implants using hydroprocessing and evaluation of their osteoconductivity," Bioinorganic chemistry and applications, vol. 2012, 2012.

[3] A. Ramos, A. Completo, C. Relvas, and J. Simões, "Design process of a novel cemented hip femoral stem concept," Materials & Design, vol. 33, pp. 313-321, 2012.

[4] H. El-Sheikh, B. MacDonald, and M. Hashmi, "Material selection in the design of the femoral component of cemented total hip replacement," Journal of materials processing technology, vol. 122, pp. 309-317, 2002.

[5] H. Hedia, S. Aldousari, and N. Fouda, "Improved design of cementless hip stems using one-dimensional functionally graded materials," METALL-BERLIN-, vol. 61, p. 129, 2007.

[6] H. Hedia, M. Shabara, T. El-Midany, and N. Fouda, "A method of material optimization of cementless stem through functionally graded material," International Journal of Mechanics and Materials in Design, vol. 1, pp. 329-346, 2004.

[7] H. Hedia, M. Shabara, T. El ‐ Midany, and N. Fouda, "Improved design of cementless hip stems using two ‐ dimensional functionally graded materials," Journal of Biomedical Materials Research Part B: Applied Biomaterials, vol. 79, pp. 42-49, 2006.

[8] F. F. Al-Jassir, H. Fouad, and O. Y. Alothman, "In vitro assessment of Function Graded (FG) artificial Hip joint stem in terms of bone/cement stresses: 3D Finite Element (FE) study," Biomedical engineering online, vol. 12, p. 5, 2013.

[9] A. Oshkour, N. A. Osman, M. Bayat, R. Afshar, and F. Berto, "Three-dimensional finite element analyses of functionally graded femoral prostheses with different geometrical configurations," Materials & Design, vol. 56, pp. 998-1008, 2014.

[10] A. Oshkour, H. Talebi, S. Shirazi, Y. Yau, S. Pramanik, F. Tarlochan, et al., "Parametric study of radial functionally graded femoral prostheses with different geometries," Meccanica, vol. 50, pp. 1657-1678, 2015.
[11] A. A. Oshkour, N. A Abu Osman, M. Davoodi, Y. Yau, F. Tarlochan, W. B Wan Abas, et al., "Finite element analysis on longitudinal and radial functionally graded femoral prosthesis," International journal for numerical methods in biomedical engineering, vol. 29, pp. 1412-1427, 2013.
[12] A. AtaollahiOshkour, H. Talebi, S. F. SeyedShirazi, M. Bayat, Y. H. Yau, F. Tarlochan, et al., "Comparison of various functionally graded femoral prostheses by finite element analysis," The Scientific World Journal, vol. 2014, 2014.
[13] A. Oshkour, N. A. Osman, Y. Yau, F. Tarlochan, and W. W. Abas, "Design of new generation femoral prostheses using functionally graded materials: a finite element analysis," Proceedings of the Institution of Mechanical Engineers, Part H: Journal of Engineering in Medicine, p. 0954411912459421, 2012.
[14] A. A. Oshkour, H. Talebi, S. Shirazi, S. Farid, Y. H. Yau, F. Tarlochan, et al., "Effect of Geometrical Parameters on the Performance of Longitudinal Functionally Graded Femoral Prostheses," Artificial organs, vol. 39, pp. 156-164, 2015.
[15] E. S. Lopes, R. J. Contieri, S. T. Button, and R. Caram, "Femoral hip stem prosthesis made of graded elastic modulus metastable β Ti Alloy," Materials & Design, vol. 69, pp. 30-36, 2015.
[16] M. Durat, M. Kapsiz, E. Nart, F. Ficici, and A. Parlak, "The effects of coating materials in spark ignition engine design," Materials & Design, vol. 36, pp. 540-545, 2012.
[17] B. Chambers, S. F. S. Clair, and M. I. Froimson, "Hydroxyapatite-coated tapered cementless femoral components in total hip arthroplasty," The Journal of arthroplasty, vol. 22, pp. 71-74, 2007.
[18] M.-S. Park, B.-W. Choi, S.-J. Kim, and J.-H. Park, "Plasma spray-coated Ti femoral component for cementless total hip arthroplasty," The Journal of arthroplasty, vol. 18, pp. 626-630, 2003.
[19] W. N. Capello, J. A. D'Antonio, M. T. Manley, and J. R. Feinberg, "Bioceramics in Total Hip Arthoplasty: Hydroxyapatite Coating," in Seminars in Arthroplasty, 2006, pp. 153-160.
[20] V. M. Ievlev, "Coatings based on calcium phosphates for metallic medical implants," Russian Chemical Reviews, vol. 82, p. 131, 2013.
[21] S. Zhang, Y. Wang, X. Zeng, K. Cheng, M. Qian, D. Sun, et al., "Evaluation of interfacial shear strength and residual stress of sol–gel derived fluoridated hydroxyapatite coatings on Ti6Al4V substrates," Engineering Fracture Mechanics, vol. 74, pp. 1884-1893, 2007.
[22] G. Singh, H. Singh, and B. S. Sidhu, "In vitro corrosion investigations of plasma-sprayed hydroxyapatite and hydroxyapatite-calcium phosphate coatings on 316L SS," Bulletin of Materials Science, vol. 37, pp. 1519-1528, 2014.
[23] P. V. Rattan, T. Sidhu, and M. Mittal, "An Overview of Hydroxyapatite Coated Titanium Implants," Asian Journal of Engineering and Applied Technology, vol. 1, pp. 40-43, 2012.
[24] G. Singh, H. S. Sidhub, B. S. Sidhuc, and B. Sabo, "A Review on Thermal Sprayed Hydroxyapatite Coated Bio-implants."
[25] R. A. Surmenev, M. A. Surmeneva, and A. A. Ivanova, "Significance of calcium phosphate coatings for the enhancement of new bone osteogenesis–A review," Actabiomaterialia, vol. 10, pp. 557-579, 2014.
[26] C. Garcia, S. Cere, and A. Duran, "Bioactive coatings deposited on titanium alloys," Journal of non-crystalline solids, vol. 352, pp. 3488-3495, 2006.
[27] Y. Xie, H. Li, C. Zhang, X. Gu, X. Zheng, and L. Huang, "Graphene-reinforced calcium silicate coatings for load-bearing implants," Biomedical Materials, vol. 9, p. 025009, 2014.
[28] S. Evans and P. Gregson, "Numerical optimization of the design of a coated, cementless hip prosthesis," Journal of Materials Science: Materials in Medicine, vol. 5, pp. 507-510, 1994.
[29] S. Sobieszczyk, W. Wojnicz, and B. Nowak, "FEM approach to estimate the behaviour of biocomposite metal-surface coating systems," Advances in Materials Sciences, vol. 8, pp. 166-172, 2008.
[30] H. Hedia and N. Fouda, "Design optimization of cementless hip prosthesis coating through functionally graded material," Computational Materials Science, vol. 87, pp. 83-87, 2014.
[31] H. S. Hedia and N. Fouda, "Improved Stress Shielding of a Coated Cemented Hip Stem by Functionally Graded Materials," Materials Testing, vol. 56, pp. 1021-1028, 2014.
[32] B. Latham and T. Goswami, "Effect of geometric parameters in the design of hip implants paper IV," Materials & design, vol. 25, pp. 715-722, 2004.
[33] E. Pyburn and T. Goswami, "Finite element analysis of femoral components paper III–hip joints," Materials & design, vol. 25, pp. 705-713, 2004.
[34] O. Kayabasi and F. Erzincanli, "Finite element modelling and analysis of a new cemented hip prosthesis," Advances in Engineering Software, vol. 37, pp. 477-483, 2006.
[35] M. Pérez, J. Garcia-Aznar, M. Doblare, B. Seral, and F. Seral, "A comparative FEA of the debonding process in different concepts of cemented hip implants," Medical engineering & physics, vol. 28, pp. 525-533, 2006.
[36] O. Kayabasi and B. Ekici, "The effects of static, dynamic and fatigue behavior on three-dimensional shape optimization of hip prosthesis by finite element method," Materials & design, vol. 28, pp. 2269-2277, 2007.
[37] A. Z. Senalp, O. Kayabasi, and H. Kurtaran, "Static, dynamic and fatigue behavior of newly designed stem shapes for hip prosthesis using finite element analysis," Materials & design, vol. 28, pp. 1577-1583, 2007.
[38] O. Kayabasi and B. Ekici, "Probabilistic design of a newly designed cemented hip prosthesis using finite element method," Materials & Design, vol. 29, pp. 963-971, 2008.
[39] A. L. Sabatini and T. Goswami, "Hip implants VII: Finite element analysis and optimization of cross-sections," Materials & Design, vol. 29, pp. 1438-1446, 2008.
[40] A. Ramos and J. Simões, "The influence of cement mantle thickness and stem geometry on fatigue damage in two different cemented hip femoral prostheses," Journal of biomechanics, vol. 42, pp. 2602-2610, 2009.
[41] C. Boyle and I. Y. Kim, "Comparison of different hip prosthesis shapes considering micro-level bone remodeling and stress-shielding criteria using three-dimensional design space topology optimization," Journal of biomechanics, vol. 44, pp. 1722-1728, 2011.
[42] D. Bennett and T. Goswami, "Finite element analysis of hip stem designs," Materials & design, vol. 29, pp. 45-60, 2008.
[43] D. Lin, Q. Li, W. Li, S. Zhou, and M. V. Swain, "Design optimization of functionally graded dental implant for bone remodeling," Composites Part B: Engineering, vol. 40, pp. 668-675, 10// 2009.
[44] A. Sadollah and A. Bahreininejad, "Optimum gradient material for a functionally graded dental implant using metaheuristic algorithms," Journal of the Mechanical Behavior of Biomedical Materials, vol. 4, pp. 1384-1395, 10// 2011.
[45] B. Henriques, S. Gonçalves, D. Soares, and F. S. Silva, "Shear bond strength comparison between conventional porcelain fused to metal and new functionally graded dental restorations after thermal–mechanical cycling," Journal of the Mechanical Behavior of Biomedical Materials, vol. 13, pp. 194-205, 9// 2012.
[46] T. A. Enab, "A comparative study of the performance of metallic and FGM tibia tray components in total knee replacement joints," Computational Materials Science, vol. 53, pp. 94-100, 2// 2012.
[47] T. A. Enab and N. E. Bondok, "Material selection in the design of the tibia tray component of cemented artificial knee using finite element method," Materials & Design, vol. 44, pp. 454-460, 2013.
[48] T. A. Enab, "Performance Improvement of Total Knee Replacement Joint through Bidirectional Functionally Graded Material," IJMME-IJENS, vol. 14, pp. 104-113, 2014.
[49] M. Bahraminasab, B. Sahari, K. L. Edwards, F. Farahmand, T. S. Hong, and H. Naghibi, "Material tailoring of the femoral component in a total knee replacement to reduce the problem of aseptic loosening," Materials & Design, vol. 52, pp. 441-451, 2013.
[50] M. Bahraminasab, B. Sahari, K. L. Edwards, F. Farahmand, T. S. Hong, M. Arumugam, et al., "Multi-objective design optimization of functionally graded material for the femoral component of a total knee replacement," Materials & Design, vol. 53, pp. 159-173, 2014.
[51] M. Nemat-Alla, "Reduction of thermal stresses by developing two-dimensional functionally graded materials," International Journal of Solids and Structures, vol. 40, pp. 7339-7356, 2003.
[52] A. Lynn and D. DuQuesnay, "Hydroxyapatite-coated Ti–6Al–4V: Part 1: the effect of coating thickness on mechanical fatigue behaviour," Biomaterials, vol. 23, pp. 1937-1946, 2002.
[53] M. T. Tilbrook, R. J. Moon, and M. Hoffman, "Finite element simulations of crack propagation in functionally graded materials under flexural loading," Engineering Fracture Mechanics, vol. 72, pp. 2444-2467, 11// 2005.